


# The *RyR2-P2328S* mutation downregulates $\text{Na}_v1.5$ producing arrhythmic substrate in murine ventricles

Feifei Ning<sup>1</sup> · Ling Luo<sup>1</sup> · Shiraz Ahmad<sup>2</sup> · Haseeb Valli<sup>2</sup> · Kamalan Jeevaratnam<sup>3,4</sup> · Tingzhong Wang<sup>1,5,6</sup> · Laila Guzadhur<sup>7,8</sup> · Dandan Yang<sup>1</sup> · James A. Fraser<sup>2</sup> · Christopher L.-H. Huang<sup>2,7</sup> · Aiqun Ma<sup>1,5,6</sup> · Samantha C. Salvage<sup>2</sup> 

Received: 19 July 2015 / Revised: 25 September 2015 / Accepted: 19 October 2015 / Published online: 6 November 2015  
© The Author(s) 2015. This article is published with open access at Springerlink.com

**Abstract** Catecholaminergic polymorphic ventricular tachycardia (CPVT) predisposes to ventricular arrhythmia due to altered  $\text{Ca}^{2+}$  homeostasis and can arise from ryanodine receptor (*RyR2*) mutations including *RyR2-P2328S*. Previous reports established that homozygotic murine *RyR2-P2328S* (*RyR2<sup>S/S</sup>*) hearts show an atrial arrhythmic phenotype associated with reduced action potential (AP) conduction velocity and sodium channel ( $\text{Na}_v1.5$ ) expression. We now relate ventricular arrhythmogenicity and slowed AP conduction in *RyR2<sup>S/S</sup>* hearts to connexin-43 (Cx43) and  $\text{Na}_v1.5$  expression and  $\text{Na}^+$  current ( $I_{\text{Na}}$ ). Stimulation protocols applying extrasystolic S2 stimulation following 8 Hz S1 pacing at progressively decremented S1S2 intervals confirmed an arrhythmic tendency despite unchanged ventricular effective refractory periods (VERPs) in Langendorff-perfused *RyR2<sup>S/S</sup>* hearts. Dynamic pacing imposing S1 stimuli then demonstrated that progressive reductions of basic cycle lengths (BCLs)

produced greater reductions in conduction velocity at equivalent BCLs and diastolic intervals in *RyR2<sup>S/S</sup>* than WT, but comparable changes in AP durations ( $\text{APD}_{90}$ ) and their alternans. Western blot analyses demonstrated that Cx43 protein expression in whole ventricles was similar, but  $\text{Na}_v1.5$  expression in both whole tissue and membrane fractions were significantly reduced in *RyR2<sup>S/S</sup>* compared to wild-type (WT). Loose patch-clamp studies similarly demonstrated reduced  $I_{\text{Na}}$  in *RyR2<sup>S/S</sup>* ventricles. We thus attribute arrhythmogenesis in *RyR2<sup>S/S</sup>* ventricles resulting from arrhythmic substrate produced by reduced conduction velocity to downregulated  $\text{Na}_v1.5$  reducing  $I_{\text{Na}}$ , despite normal determinants of repolarization and passive conduction. The measured changes were quantitatively compatible with earlier predictions of linear relationships between conduction velocity and the peak  $I_{\text{Na}}$  of the AP but nonlinear relationships between peak  $I_{\text{Na}}$  and maximum  $\text{Na}^+$  permeability.

Feifei Ning and Ling Luo contributed equally as the first authors.  
Christopher L.-H. Huang, Aiqun Ma and Samantha C. Salvage contributed equally as the senior authors.

✉ Aiqun Ma  
maaiqun@medmail.com.cn

✉ Samantha C. Salvage  
ss2148@cam.ac.uk

<sup>1</sup> Department of Cardiovascular Medicine, First Affiliated Hospital of Xi'an Jiaotong University, No. 277 West Yanta Road, Xi'an, Shaanxi 710061, People's Republic of China

<sup>2</sup> Physiological Laboratory, University of Cambridge, Cambridge CB2 3EG, UK

<sup>3</sup> Faculty of Health and Medical Science, Duke of Kent Building, University of Surrey, Guildford GU2 7TE, UK

<sup>4</sup> Perdana University-Royal College of Surgeons Ireland, 43400 Serdang, Selangor Darul Ehsan, Malaysia

<sup>5</sup> Key Laboratory of Molecular Cardiology, Shaanxi Province, People's Republic of China

<sup>6</sup> Key Laboratory of Environment and Genes Related to Diseases (Xi'an Jiaotong University), Ministry of Education, Xi'an, People's Republic of China

<sup>7</sup> Department of Biochemistry, University of Cambridge, Cambridge CB2 1QW, UK

<sup>8</sup> Niche Science and Technology, Falstaff House, Bardolph Road, Richmond, UK

**Keywords** RyR2 · CPVT · Na<sub>v</sub>1.5 · Arrhythmogenicity · Conduction velocity · Ca<sup>2+</sup> homeostasis

## Introduction

Catecholaminergic polymorphic ventricular tachycardia (CPVT) is an inherited arrhythmic syndrome characterized by episodic syncope and/or sudden cardiac arrest, typically triggered by adrenergic stimulation as occurs during strenuous exercise or emotional stress [1, 34, 46]. CPVT has been associated with mutations in various Ca<sup>2+</sup> handling proteins, which lead to abnormalities in Ca<sup>2+</sup> homeostasis; most notably, these mutations are found in the cardiac ryanodine receptor-Ca<sup>2+</sup> release channel (RyR2) [25, 35] and the sarcoplasmic reticulum (SR) Ca<sup>2+</sup>-binding protein calsequestrin 2 (CASQ2) [13, 19]. Ca<sup>2+</sup>-dependent calmodulin missense mutations also occur in a small number of cases [18]. Some RyR2 mutations also predispose to atrial arrhythmias [4, 34, 39]. For example, the RyR2-P2328S mutation is associated with high incidences of both CPVT and atrial tachycardia (AT) [25, 37, 40]. This RyR2 variant has been associated with a normal luminal SR Ca<sup>2+</sup> release sensitivity but an increased sensitivity to cytosolic Ca<sup>2+</sup> [31], giving rise to lower cytosolic Ca<sup>2+</sup> thresholds leading to Ca<sup>2+</sup> release. If reached during increased heart rates, these could be sufficient to elicit a ‘leak’ of SR Ca<sup>2+</sup> consequently triggering arrhythmia.

The atrial and ventricular phenotypes are replicated by the RyR2-P2328S (RyR2<sup>S/S</sup>) murine model which shows potential arrhythmic triggers in the form of delayed after-depolarizations [15, 22]. However, there remains a requirement for an electrophysiological tissue substrate in order to perpetuate and sustain arrhythmia, which has previously been typified by a reduced conduction velocity ( $\theta$ ) in systems showing reduced Na<sub>v</sub>1.5 expression [33], connexin 40 and/or 43 (atria) or connexin 43 (ventricle) expression [16, 23], or structural abnormalities, including fibrosis [44]. Interestingly, several reports have indicated the potential for Na<sub>v</sub>1.5 expression [6, 11, 42] and function [2, 41] to be modulated, both directly and indirectly, by alterations in cytosolic Ca<sup>2+</sup>. Rat cardiomyocytes showed reductions in Na<sup>+</sup> channel activity following imposed increases of intracellular [Ca<sup>2+</sup>]. Additionally, the Ca<sup>2+</sup> channel blocker verapamil and the Ca<sup>2+</sup> ionophore calcimycin increased and decreased Na<sub>v</sub>1.5 mRNA and Na<sub>v</sub>1.5 protein expression respectively [11, 42]. In agreement with these findings, elevations and reductions of cytosolic [Ca<sup>2+</sup>], by chronic treatment with high extracellular [Ca<sup>2+</sup>] and [K<sup>+</sup>] or BAPTA-AM, decreased and increased Na<sup>+</sup> current densities, respectively [6]. More recently, Casini et al. [5] demonstrated that acute increases in pipette [Ca<sup>2+</sup>] were capable of reducing both Na<sup>+</sup> current density and (dI/dt)<sub>max</sub>.

Biochemical evidence accounting for the potential mechanisms of functional modulation of Na<sub>v</sub>1.5 by cytosolic [Ca<sup>2+</sup>] identifies both direct and indirect Ca<sup>2+</sup> binding sites on

Na<sub>v</sub>1.5. Direct Ca<sup>2+</sup> binding to Na<sub>v</sub>1.5 is mediated at an EF hand motif resident at the carboxy-terminal region of Na<sub>v</sub>1.5 [47]. This binding results in a depolarizing shift of the voltage dependence of Na<sup>+</sup> channel inactivation with a potential increase in Na<sup>+</sup> channel activity [47]. Indirect mechanisms of Ca<sup>2+</sup> binding have been attributed to both the presence of an additional binding site, the ‘IQ’ domain, within the C-terminal region of Na<sub>v</sub>1.5 for Ca<sup>2+</sup>/Calmodulin (Ca<sup>2+</sup>/CaM) and multiple phosphorylatable sites (including serines 516 and 571 and threonine 594) within the IDI-II linker region of Na<sub>v</sub>1.5 targeted by Ca<sup>2+</sup>/CaM Kinase II (CaMKII). These two mechanisms occur only subsequent to Ca<sup>2+</sup> binding to the EF hand motifs of Ca<sup>2+</sup>/Calmodulin (Ca<sup>2+</sup>/CaM) or Ca<sup>2+</sup>/CaM Kinase II (CaMKII) and thus constitutes an indirect interaction of Ca<sup>2+</sup> with Na<sub>v</sub>1.5. Ca<sup>2+</sup>/CaM binding at the IQ domain and CaMKII-dependent phosphorylation shifts Na<sup>+</sup> current availability to a more depolarized membrane potential [2] and enhances slow inactivation of the Na<sup>+</sup> current [41].

Recent reports have indeed implicated reduced Na<sub>v</sub>1.5 expression and Na<sup>+</sup> channel function in the increased arrhythmogenicity in RyR2<sup>S/S</sup> atria [21, 22, 36]. They also demonstrated a reduced conduction velocity [22], resulting from a reduced Na<sup>+</sup> current attributable either to a reduced Na<sub>v</sub>1.5 expression or the direct inhibitory effect on Na<sup>+</sup> channel function of altered Ca<sup>2+</sup> homeostasis outlined previously. Slowed conduction resulting from reduced Na<sub>v</sub>1.5 expression would potentially produce arrhythmic substrate, which would compound the arrhythmic effect of Ca<sup>2+</sup>-mediated triggered activity in the RyR2<sup>S/S</sup> [21, 22, 36].

The present study investigates for possible roles of Cx43 expression as well as Na<sub>v</sub>1.5 expression and function in RyR2<sup>S/S</sup> ventricular, as opposed to atrial, arrhythmogenicity. First, the arrhythmic properties of the RyR2<sup>S/S</sup> ventricle compared to the WT was confirmed in accordance with earlier reports [15] and correlated with measurements of action potential duration (APD), conduction velocity ( $\theta$ ) and their alternans, as well as ventricular effective refractory period (VERP). The stimulation protocols either interposed extrasystolic, S2, stimuli at progressively decremented S1S2 intervals within 8 Hz S1 pulse trains or applied steady stimulus frequencies at progressively decremented basic cycle lengths (BCLs). Second, to assess the underlying mechanism for the slowed conduction and arrhythmic phenotype, we assessed the ventricular expression of Cx43 and Na<sub>v</sub>1.5, the latter assessed in both the whole ventricle and the membrane fraction compared between WT and RyR2<sup>S/S</sup> hearts. Third, the corresponding functional evaluation of Na<sub>v</sub>1.5 was investigated through peak I<sub>Na</sub> current recordings of WT and RyR2<sup>S/S</sup> ventricular tissue. These comparisons successfully correlated Na<sub>v</sub>1.5 expression and function, particularly within the functional Na<sub>v</sub>1.5 containing membrane fraction, with the incidence of ventricular arrhythmia, and the resulting conduction changes in RyR2<sup>S/S</sup> ventricles.

## Materials and methods

### Experimental animals

Homozygous *RyR2<sup>S/S</sup>* and WT mice (aged 4 to 6 months) with an inbred 129/Sv genetic background (supplied initially by Harlan, UK) were generated as described previously [15]. Mice were kept in plastic cages at room temperature in an animal facility, given free access to sterile rodent chow and water and subjected to 12 h light/dark cycles. Mice were killed by cervical dislocation for experimentation. All procedures conformed to the UK Animals (Scientific Procedures) Act 1986, approved by a university ethics review board. Hearts were rapidly excised and submerged in ice-cold Krebs-Henseleit (KH) buffer solution (containing, in mM, NaCl 119, NaHCO<sub>3</sub> 25, KCl 4, KH<sub>2</sub>PO<sub>4</sub> 1.2, MgCl<sub>2</sub> 1, CaCl<sub>2</sub> 1.8, glucose 10 and Napyruvate 2, pH 7.4, 95 % O<sub>2</sub>/ 5 % CO<sub>2</sub>; British Oxygen Company, Manchester, UK) for whole heart electrophysiological studies and Western blot analyses. All chemicals were purchased from Sigma-Aldrich (Poole, Dorset, UK), unless otherwise stated. Six WT and seven *RyR2<sup>S/S</sup>* mice were used in whole heart electrophysiological investigations. Four WT and four *RyR2<sup>S/S</sup>* hearts were used for Western blot studies of Cx43 expression. Seven WT and six *RyR2<sup>S/S</sup>* mice were used for Western blot studies of Na<sub>v</sub>1.5 expression in the whole tissue and membrane fraction. Four WT and three *RyR2<sup>S/S</sup>* mice were used to give *n*=6 and 12 patches, respectively, for loose patch-clamp studies of Na<sup>+</sup> currents. Male and female mice were used in statistically equal numbers in each group.

### Electrophysiological studies in whole heart

Excised hearts were cannulated and retrograde perfused on a Langendorff system as previously described [28, 29, 38, 48]. Prior to electrophysiological testing, hearts were perfused with KH solution for at least 5 min to achieve a steady state. Monophasic action potentials (MAPs) were recorded by microMAP electrodes (HugoSachs, Harvard Apparatus, UK) placed upon the epicardial surface. Recordings were amplified (Neurolog NL100 preamplifier; NL104 amplifier, Digitimer, Welwyn Garden City, UK), band-pass filtered (NL125/126 filter; 0.5 Hz to 1.0 kHz) and sampled at 5 kHz (micro1401 interface) for display using Spike2 software (Cambridge Electronic Design, Cambridge, UK).

Hearts were paced at twice their excitation threshold voltage using a bipolar platinum-coated stimulating electrode placed on the ventricular septum connected to a DS2A-Mk.II stimulator (Digitimer). After pacing at 8 Hz for at least 5 min to attain and confirm a steady state, two types of pacing protocols were applied. A S1S2 protocol first stimulated hearts at frequencies of 10 Hz for 20 s; this was followed by cycles of drive trains of eight S1 beats delivered at 8 Hz followed by an S2 extra-stimulus, at S1-S2 coupling interval successively

reduced by 1 ms with each subsequent cycle until either 2:1 block or sustained arrhythmia occurred. A dynamic pacing protocol [24, 28, 29] first assessed action potential (AP) properties at a BCLs of 134 ms duration for 100 stimulations. The BCL was then decremented by 5 ms, and the pacing sequence repeated until the hearts showed either entry into 2:1 block or sustained arrhythmia. Both stimulation protocols yielded incidences of arrhythmia. The S1S2 protocol additionally provided VERPs. The dynamic pacing protocol yielded APDs, and an indication of conduction velocity  $\theta'$  (1/latency, which was measured as the time from the stimuli to the peak of the MAP) as a function of BCL, measured as the recovery time from AP peak to 90 % full repolarization, APD<sub>90</sub> (Fig. 1). The corresponding diastolic intervals (DIs) were calculated from the BCL and APD<sub>90</sub> values using the relationship:

$$DI = BCL - APD_{90}$$

### Protein extraction and Western blot analysis

The method of protein extraction was optimized for the protein of interest. For connexin proteins, which are primarily found in the surface membrane in hexameric clusters, a well-established high content sodium dodecyl sulphate (SDS) buffer [7, 12, 43] was used in order to fully solubilize the membrane and maximize release of the connexin proteins from the gap junction channels in the plasma membrane. For Na<sub>v</sub>1.5 channels, we chose to use a milder buffer, followed by a centrifugation step and solubilization in order to separate out the membrane and non-membrane fractions based on the different distribution and abundance of Nav1.5 channels and their contribution to conduction.

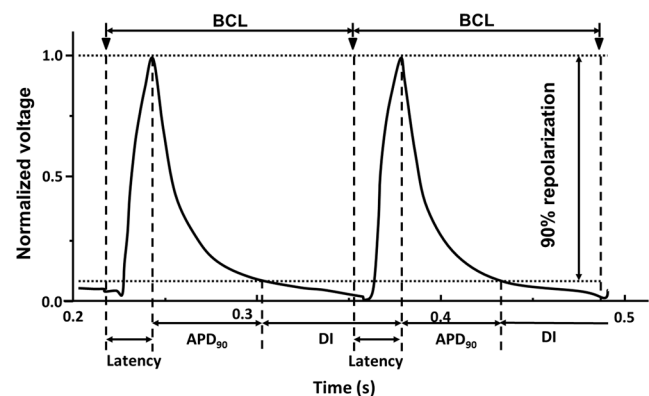


**Fig. 1** Two typical successive monophasic action potential (MAP) recordings at the LV epicardium of a WT heart obtained during dynamic pacing to highlight the derivation of the various parameters used for analysis; BCL, latency, APD<sub>90</sub> and DI. BCL was the time interval between the adjacent stimuli, thus the pacing rate. Latency was measured as the time elapsed from the stimuli to the peak of MAP. APD<sub>90</sub> is the time course over which 90 % repolarization of the MAPs obtained. DI was measured as BCL-APD<sub>90</sub>, thus comprising the final 10 % of MAP repolarization and up to the start of the next stimuli

Ventricular tissues of the excised hearts were snap-frozen and crushed into powder by a clamp pre-cooled with liquid  $N_2$ . The powdered tissue was homogenized in either SB20 (20 % SDS, 2 mM EDTA, 150 mM Tris) [7, 12, 43] and diluted to an appropriate gel loading concentration in sample loading buffer (90 % SB20, 5 % 2-mercaptoethanol, 5 % w/v bromophenol blue) for connexin 43 analysis, or the re-suspension buffer (containing, in mM, Tris-HCl 50, NaCl 10, Sucrose 320, EDTA 5, EGTA 2.5 and Protease inhibitors (1 tablet/20 ml; Roche, West Sussex, UK), pH 7.4) and lysis buffer (containing, in mM, Tris-HCl 20, EDTA 2, NaCl 137 and Triton X-100 1 %, glycerol 10 %, pH 7.4) and then centrifuged for 15 min at 13,000g and 4 °C for  $Na_v1.5$  analysis. The supernatant was divided into two parts. One was stored at -80 °C as the whole tissue fraction and the rest was centrifuged at 100,000g at 4 °C for an hour to extract the membrane proteins. The pellet was re-suspended in radioimmunoprecipitation assay (RIPA) lysis buffer and then vortexed and placed on ice for 30 min to harvest the membrane protein.

For Western blot analysis, the protein extracts from whole tissue and the membrane fraction were separated on premade 4–12 % Bis-Tris Gels (Invitrogen, Paisley, UK) and then transferred onto PVDF membranes (Immobilon-P, Millipore, Hertfordshire, UK). Blots were blocked in 5 % skimmed milk in TBST (Tris-buffered saline; Invitrogen, Paisley, UK and Tween 20) and then probed with either anti- $Na_v1.5$  (rabbit anti-mouse IgG, 1:1000, Alomone, Jerusalem, Israel) or anti-Cx43 (rabbit anti-mouse, 1:10,000, C6219 Sigma-Aldrich) and anti-GAPDH (Abcam, Cambridge, UK) or anti- $\alpha$ -tubulin (Cell Signaling Technology, Danvers, MA, USA) antibodies overnight at 4 °C. Horseradish peroxidase (HRP)-conjugated secondary antibody (Abcam, 1:10000 to 1:50000) were detected using an enhanced chemiluminescent system (GE Healthcare, Little Chalfont, Bucks, UK). Specific protein bands were quantified using Image J (National Institutes of Health, Wash., USA).

### Loose patch clamp recordings of $I_{Na}$ in ventricular tissue

Loose patch clamp experiments previously described for atrial tissue [21, 36] were performed in a right ventricular tissue preparation. This technique allows for measurement of  $Na^+$  currents in whole, perfused ventricular tissue preparations where intracellular  $Ca^{2+}$  homeostasis is not disrupted by cell isolation. Furthermore, the tissue preparation allows a more reliable comparison with APD<sub>90</sub> and CV measurements of this study. Activation properties were assessed in order to determine peak  $I_{Na}$ . The activation protocol utilized a series of 75 ms duration depolarizing pulses, incremented by 10 mV steps ranging from 20 to 120 mV excursions applied 5 ms after the beginning of the sampling period using a P/4 pulse protocol [3].

### Statistical analysis

Statistical analysis for differences between experimental groups was performed using Graphpad Prism software (La Jolla, CA 92037 USA), applying unpaired Student's *t* tests. A value of  $P < 0.05$  was considered statistically significant. Data are presented as means  $\pm$  SEM.

## Results

### Comparison of ventricular arrhythmogenicity in S1S2 protocols and dynamic protocols

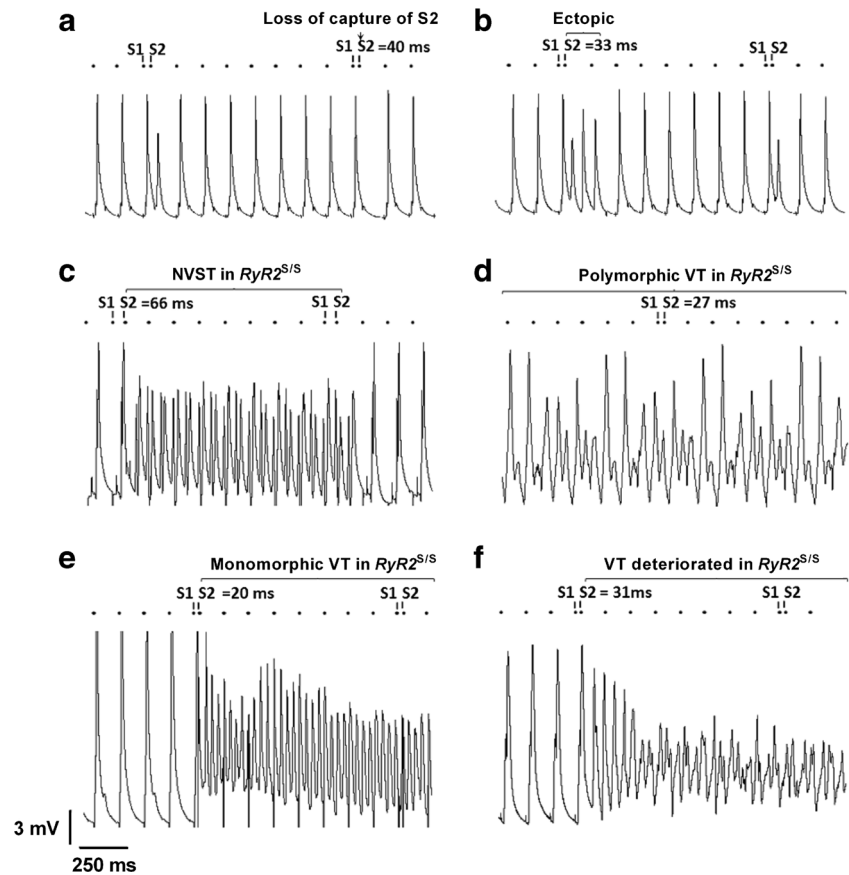
We initially confirmed the arrhythmogenic phenotype of the  $RyR2^{S/S}$  murine heart as previously reported [15]. An S1S2 stimulation protocol was used to determine the incidence, frequency and duration of ventricular arrhythmia in isolated Langendorff-perfused hearts.

The occurrence of ventricular tachycardia (VT) was defined as an occurrence of two or more sequential spontaneous APs, as in previous work [36] in the course of programmed electrical stimulation. Figure 2 illustrates representative left ventricular epicardial traces from WT (A, B) and  $RyR2^{S/S}$  (C–F) hearts, displaying regular activity (A), ectopic (B) and VT (C–E) and ventricular fibrillation (VF) (F) episodes during the S1S2 protocol. Six WT and seven  $RyR2^{S/S}$  hearts were subject to the S1S2 protocol described in methods. None of the WT hearts showed VT, although one heart showed three separate ectopic events (at S1S2 intervals of 33, 31 and 30 ms). In contrast, the  $RyR2^{S/S}$  hearts showed 30 episodes of arrhythmia, taking the form of either polymorphic or monomorphic VT in three of the hearts. Of these hearts, the first showed 7 episodes of VT, lasting approximately 2.8 s, with an additional VT episode that degenerated into VF lasting approximately 22.5 s. The second heart showed one episode of VT lasting approximately 11.2 s. The third heart showed 21 episodes of VT accounting for a total time of approximately 14 s.

Ventricular effective refractory periods (VERPs) were defined as the time period during which the myocardium is incapable of re-excitation in response to the twice-threshold stimulus employed in the S1S2 protocols [10, 32]. It was thus the S1S2 interval at which loss of S2 capture first occurred in an absence of VT. WT and  $RyR2^{S/S}$  hearts typically became refractory at similar S1S2 pacing intervals (VERP: WT:  $38.2 \pm 1.55$  ms ( $n=6$ );  $RyR2^{S/S}$ :  $37.5 \pm 5.04$  ms ( $n=5$ );  $P=0.9057$ ). VERP could not be ascertained from all the mice studied due to arrhythmogenesis: sustained arrhythmias occurred in two of the seven  $RyR2^{S/S}$  hearts during the S1S2 protocol.

The differing arrhythmic properties of WT and  $RyR2^{S/S}$  were further confirmed in the dynamic pacing protocol,

**Fig. 2** MAP traces obtained from the epicardium of the left ventricle in WT and *RyR2<sup>S/S</sup>* hearts during S1S2 pacing highlighting typical traces of either normal activity or arrhythmogenesis. All WT hearts entered the refractory period without displaying any episodes of arrhythmia, as defined by two or more non-stimulated APs (a); however, one heart displayed the occurrence of a singular ectopic (one non-stimulated AP) (b). Multiple arrhythmic events were observed in *RyR2<sup>S/S</sup>* hearts including short non-sustained ventricular tachycardia (NSVT) (c), polymorphic tachycardia following a previously imposed S2 extrastimulus (d), monomorphic ventricular tachycardia (VT) (e) and episodes of VT which deteriorated into ventricular fibrillation (VF) (f). The small black circles indicate the timing of stimuli



which subjected hearts to systematically decreasing BCLs. Two of the six WT hearts showed VT at BCLs of 39 and 44 ms. However, these correspond to BCLs which are substantially lower, thus a much higher heart rate than those experienced during normal physiological maximal exercise [8]. *RyR2<sup>S/S</sup>* hearts not only demonstrated higher incidences of VT and VF but they occurred also at higher BCLs than WT (54, 64, 54 and 74 ms in four *RyR2<sup>S/S</sup>* hearts respectively; these necessitated termination of the protocol, suggesting a reduced capacity to tolerate increased heart rates as may be observed during emotional or physical stress such as exercise [8].

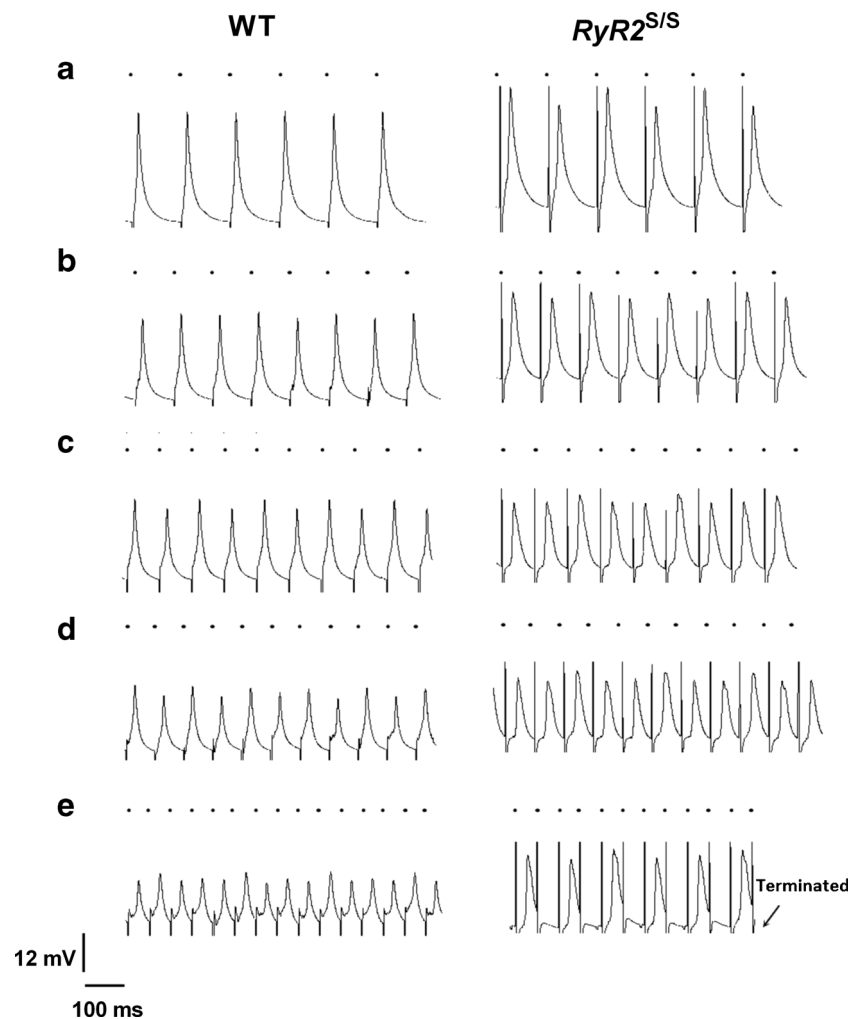
### Action potential properties and conduction at varying pacing rates

AP propagation and recovery properties at different BCLs were then investigated using the dynamic pacing protocol. Figure 3 illustrates typical APs thus obtained from the LV epicardium of WT (left column) and *RyR2<sup>S/S</sup>* hearts (right column). In both cases, AP amplitude decreased with increasing pacing rate in every heart, independent of genotype (Fig. 3a–e). At lower pacing rates, *RyR2<sup>S/S</sup>* hearts showed a higher incidence of alternans (Fig. 3a, right column) compared with WT hearts (Fig. 3c, left column). Around half of both the

WT and the *RyR2<sup>S/S</sup>* hearts had shown either a loss of capture or arrhythmogenesis when the BCL reached 54 ms (Fig. 3e).

Figure 4 plots averaged (mean±SEM)  $APD_{90}$  (A, C) and  $\theta'$  ( $=1/\text{latency}$ ) (B, D) values in WT (filled symbols) and *RyR2<sup>S/S</sup>* (open symbols) hearts against BCL (A, B) and DI (C, D). At BCLs, where significant differences between readings at the two genotypes were obtained, this is indicated ( $*P<0.05$ ;  $**P<0.01$ ). Both WT and *RyR2<sup>S/S</sup>* showed similar ( $P>0.05$ ) values of  $APD_{90}$  at each BCL and DI. These both declined with decreasing BCL and DI. *RyR2<sup>S/S</sup>* and WT hearts additionally showed 2:1 block at similar values of BCL (WT  $56.5 \pm 5.95$  ms,  $n=4$ ; *RyR2<sup>S/S</sup>*:  $54 \pm 2.5$  ms,  $n=3$ ;  $P=0.751$ ). As with VERP for the S1S2 protocol, 2:1 block was not obtained from all the mice studied; this was due to arrhythmogenesis warranting termination of the dynamic pacing protocol in four of the seven *RyR2<sup>S/S</sup>* hearts and two of six WT hearts. In contrast to similar  $APD_{90}$ , at equivalent BCLs, *RyR2<sup>S/S</sup>* hearts showed consistently lower  $\theta'$  than WT hearts at equivalent BCLs. Indeed, the highest mean  $\theta'$  showed by the *RyR2<sup>S/S</sup>* ( $0.043 \pm 0.003$  m s<sup>-1</sup>), which was observed at the highest BCL, was similar to the lowest  $\theta'$  ( $0.042 \pm 0.006$  m s<sup>-1</sup>) shown by the WT, which was observed at the shortest BCLs. These findings were corroborated when the  $APD_{90}$  and  $\theta'$  values were plotted against their preceding DIs reflecting recovery times from the preceding APs (C, D). The present findings

**Fig. 3** Typical MAP recordings obtained from the left ventricular epicardium of WT and  $RyR2^{S/S}$  during dynamic pacing. Traces from WT (*left*) and  $RyR2^{S/S}$  at progressively decreasing BCLs: 124 (a), 99 (b), 84 (c), 74 (d) and 54 ms (e). If a heart entered 2:1 block, the protocol was terminated (E). Traces are displayed along a common horizontal timescale. The vertical scale was normalized to a standard AP deflection at a BCL of 134 ms. *Small black circles* above each trace indicate the timing of stimuli



demonstrate normal AP repolarization characteristics, but compromised AP conduction in the  $RyR2^{S/S}$  arrhythmic phenotype, which could arise from abnormalities in gap junction channels and/or  $Na_v1.5$ .

Alternans of electrophysiological parameters, reflecting temporal variability, often presages arrhythmic activity. Figure 5 assesses the average (mean $\pm$ SEM) degree of alternans in AP amplitude (A, D) [30],  $APD_{90}$  (B, E) and  $\theta'$  (C, F) at different BCLs (A–C) and DIs (D–F) in WT (filled symbols) and  $RyR2^{S/S}$  (open symbols) hearts. Alternans reflects system instability through the mean difference between alternating high and low values of a given parameter normalized to the mean value of the parameter. Both the  $RyR2^{S/S}$  and the WT demonstrated similarly increasing AP amplitude instabilities with either decreasing BCL or decreasing DI.  $RyR2^{S/S}$  and WT showed similar  $APD_{90}$  and  $\theta'$  instabilities which similarly varied with decreasing BCL or DI.  $\theta'$  instabilities were relatively small in contrast to the large changes in their mean values described.

These findings implicate abnormal conduction as opposed to abnormal repolarization in the  $RyR2^{S/S}$  ventricular arrhythmic phenotype. The underlying mechanism/cause of this abnormal conduction is thus investigated in the next sections.

#### Cx43 expression is comparable between the ventricles of WT and $RyR2^{S/S}$ murine hearts

Abnormal cardiac conduction can arise from one of three factors: abnormal connexin expression/gap junction formation, impaired Na channel function and/or structural abnormalities such as with fibrosis or hypertrophy. Due to the structural similarity of WT and  $RyR2^{S/S}$  hearts [49], we pursued the remaining two factors.

We first assessed the expression of the ventricular gap junction protein, Cx43. Western blots of whole tissue ventricular lysates from WT and  $RyR2^{S/S}$  hearts demonstrate that the overall expression of Cx43, normalized to the housekeeping gene glyceraldehyde 3-phosphate dehydrogenase (GAPDH), was not significantly different between

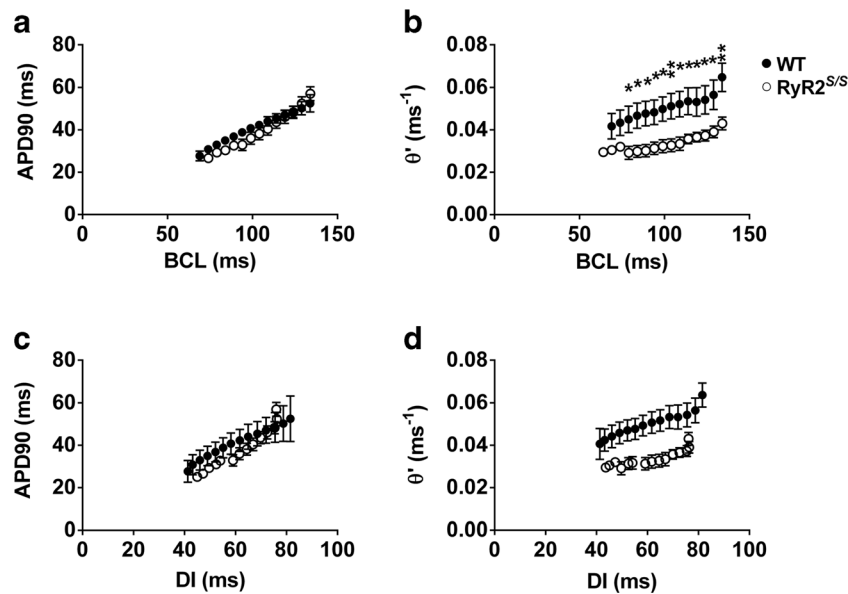


**Fig. 4** Plots of  $APD_{90}$  and  $\theta'$  at different BCLs and DIs in WT and  $RyR2^{S/S}$  hearts. **a, b** Mean ( $\pm$  SEM) values for  $APD_{90}$  and  $\theta'$  respectively at different BCLs (134, 129, 124, 119, 114, 109, 104, 99, 94, 89, 84, 79, 74 and 69 ms) for WT ( $n=6$ , filled symbols) and  $RyR2^{S/S}$  ( $n=7$ , open symbols) hearts. **c, d** Mean ( $\pm$  SEM) values for  $APD_{90}$  and  $\theta'$ , respectively, at different DIs for WT ( $n=6$ , filled symbols) and  $RyR2^{S/S}$

( $n=7$ , open symbols) hearts.  $APD_{90}$  is virtually superimposable at all BCLs between WT and  $RyR2^{S/S}$  hearts and thus shows no statistically significant variation. However,  $\theta'$  is consistently lower in  $RyR2^{S/S}$  hearts as compared to WT hearts with significant differences between the genotypes denoted by asterisks; \* $P<0.05$  and \*\* $P<0.01$

WT and  $RyR2^{S/S}$  ventricles ( $0.59\pm 0.07$ ;  $n=4$  and  $0.79\pm 0.1$ ;  $n=4$ , respectively;  $P>0.05$ , Fig. 6). This suggests that a loss of Cx43 expression is not a contributory factor to the slowed ventricular conduction and increased arrhythmogenesis observed in the ventricles of  $RyR2^{S/S}$  hearts, in parallel to findings in the atria of the same model [21].

#### Decreased $Na_v1.5$ expression in the ventricles of $RyR2^{S/S}$ murine hearts

Western blots of WT and  $RyR2^{S/S}$  ventricular homogenates (Fig. 7) illustrate a decreased  $Na_v1.5$  expression in the  $RyR2^{S/S}$  relative to the WT in both the whole tissue fraction (Fig. 7a; left panel) ( $1.17\pm 0.2$ ;  $n=6$ , and  $1.69\pm 0.15$ ;  $n=7$ , respectively;

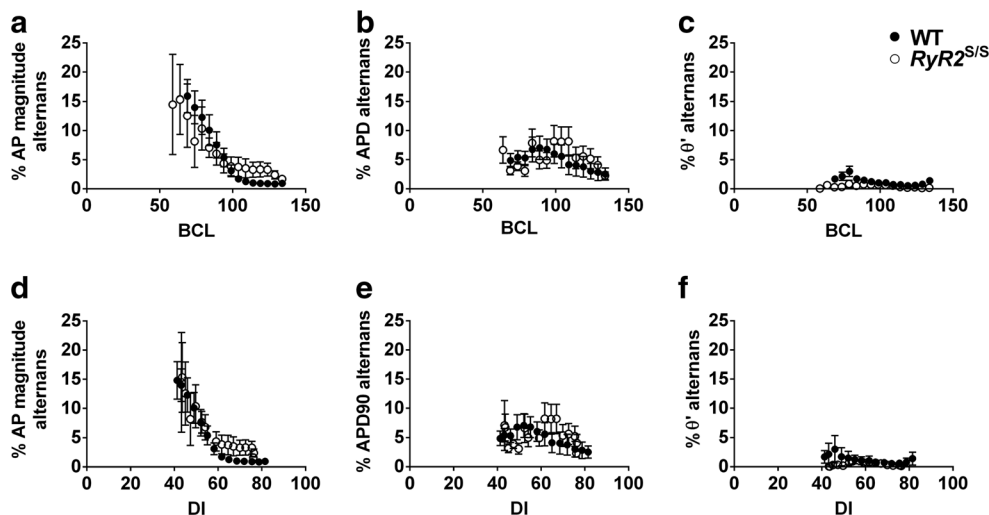


**Fig. 5** Plots of alternans at different BCLs and DIs. The mean ( $\pm$  SEM) alternans characteristics of AP amplitude (**a, d**),  $APD_{90}$  (**b, e**) and  $\theta'$  (**c, f**) for WT (filled symbols) and  $RyR2^{S/S}$  (open symbols) hearts have been plotted as percentage variation between each beat as a function of BCL (**a–c**) and DI (**d, e**) AP magnitude displays an increasing degree of

alternans with decreasing BCL and DI; however, this does not vary between genotypes. Similarly, a small degree of alternans is observed in the  $APD_{90}$  and less so the  $\theta'$  with decreasing BCL and DI, but these do not vary significantly between the WT and  $RyR2^{S/S}$  hearts

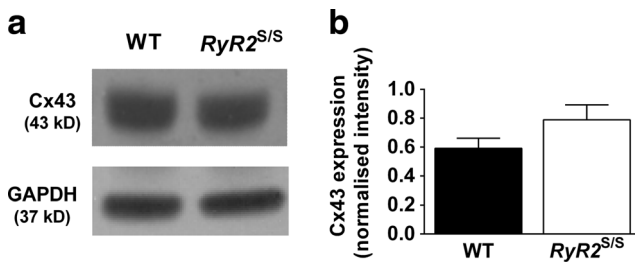


**Fig. 6** Total Cx43 expression in WT and  $RyR2^{S/S}$  ventricles. **a** Representative blots of Cx43 and GAPDH expression in WT and  $RyR2^{S/S}$  ventricular tissue and **b** the mean ( $\pm$  SEM) Cx43 expression normalized to GAPDH expression. Cx43 expression was similar between WT and  $RyR2^{S/S}$  ( $0.59 \pm 0.07$  and  $0.79 \pm 0.1$ , respectively;  $P = 0.167$ ,  $n = 4$ ) ventricles

$P < 0.05$ ) and within the membrane fraction (Fig. 7a; right panel) ( $2.06 \pm 0.33$ ;  $n = 4$ , and  $0.91 \pm 0.13$ ;  $n = 4$ , respectively;  $P < 0.01$ ). Thus,  $Na_v1.5$  expression in  $RyR2^{S/S}$  ventricles was approximately 69 % of that seen in the WT whole tissue fraction and down to only 44 % of WT in the membrane fraction (Fig. 7b). This significant reduction of  $Na_v1.5$  expression in the ventricular membrane where the function of  $Na_v1.5$  channels is crucial to cardiac excitability, and conduction would be expected to lead to a significant reduction in  $I_{Na}$  in the  $RyR2^{S/S}$  heart compared to the WT.

#### Decreased $I_{Na}$ in the ventricles of $RyR2^{S/S}$ murine hearts

To assess whether the reduced expression of  $Na_v1.5$  in  $RyR2^{S/S}$  ventricles correlated with a functional alteration of  $Na_v1.5$ , we measured  $I_{Na}$  in both WT and  $RyR2^{S/S}$  ventricles using the loose patch clamp technique. Figure 8a illustrates

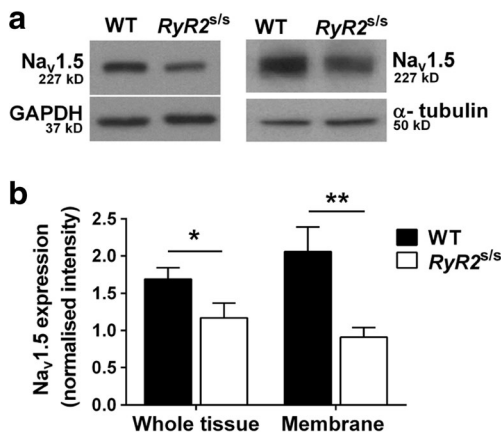


**Fig. 7** Western blots of  $Na_v1.5$  expression in whole tissue and membrane fraction samples from WT and  $RyR2^{S/S}$  ventricles. Ventricular  $Na_v1.5$  expression was decreased in  $RyR2^{S/S}$  compared to WT, both in the whole tissue ( $1.17 \pm 0.20$ ;  $n = 6$ , vs  $1.69 \pm 0.15$   $n = 7$ , respectively,  $P = 0.048$ ) and in the membrane fraction ( $0.91 \pm 0.13$ ;  $n = 4$ , vs  $2.06 \pm 0.33$ ;  $n = 4$ , respectively,  $P = 0.006$ ). This suggested a greater proportional reduction in membrane relative to total  $Na_v1.5$  expression in  $RyR2^{S/S}$ . Symbols denote significant differences between genotypes \* $P < 0.05$ , \*\* $P < 0.01$

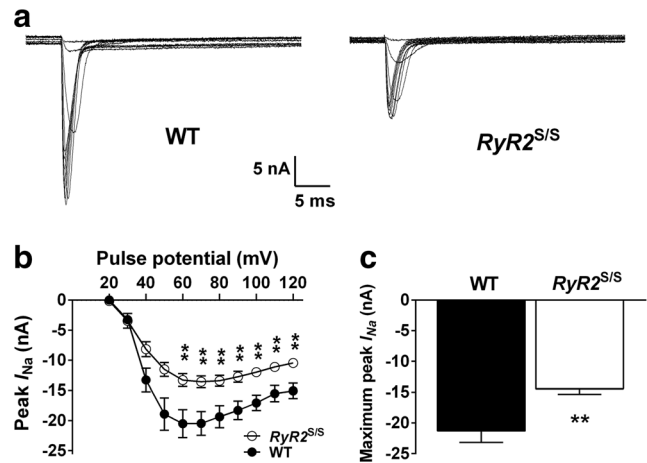


**Fig. 8** Loose patch clamp recordings of  $I_{Na}$  activation in WT and  $RyR2^{S/S}$  ventricles. **a** Representative currents in response to depolarizing steps increased from 20 to 120 mV in voltage-clamped WT and  $RyR2^{S/S}$  ventricular tissue. **b** Peak inward current (mean  $\pm$  SEM) elicited at each voltage step for WT ( $n = 6$ ) and  $RyR2^{S/S}$  ( $n = 12$ ) ventricles. **c** The maximum current recorded during each complete voltage step protocol (mean  $\pm$  SEM) was larger in the WT than the  $RyR2^{S/S}$  ventricles,  $P < 0.0047$ . The asterisks denote significant differences between genotypes of  $P < 0.01$

representative currents elicited by WT and  $RyR2^{S/S}$  ventricles following a series (20–120 mV voltage excursions) of depolarizing test pulses. The peak current elicited at each voltage excursion and the overall peak current for both WT and  $RyR2^{S/S}$  ventricles are shown in Fig. 8b, c, respectively. Currents recorded from the WT ventricle were significantly larger than those recorded in the  $RyR2^{S/S}$  ventricle at depolarizing pulses of 60 mV or greater ( $P < 0.01$ ). The overall peak current in the  $RyR2^{S/S}$  was  $-14.45 \text{ nA} \pm 0.88 \text{ nA}$  while in the WT it was  $-21.3 \text{ nA} \pm 1.87 \text{ nA}$  ( $P < 0.01$ ); this equates to a 32 % reduction in peak  $I_{Na}$  in the  $RyR2^{S/S}$ .

#### Discussion

The present experiments demonstrate that reduced  $Na_v1.5$  expression and Na current is associated with the reduced conduction velocity and consequent arrhythmic substrate and ventricular arrhythmogenesis in homozygotic murine  $RyR2-P2328S$  ( $RyR2^{S/S}$ ) hearts. The quantitative changes were compatible with earlier reports of linear relationships predicted between the conduction velocity and the peak  $I_{Na}$  of the AP, but a nonlinear (logarithmic) relationship between peak  $I_{Na}$  and maximum  $Na^+$  permeability [20]. Thus, increased arrhythmogenicity was associated with a reduced conduction velocity of  $\sim 22$  % during steady 8 Hz pacing and in the region of a  $\sim 33$  % reduction during dynamic pacing, which would correspond to comparable reductions in AP wavelength given an absence of significant changes in repolarization characteristics (VERP and  $APD_{90}$ ), and determinants of passive conduction reflected in Cx43 expression. These in turn



accompanied reductions in membrane  $\text{Na}_v1.5$  expression of ~56 % and peak  $I_{\text{Na}}$  of ~32 %.

The murine  $RyR2^{S/S}$  heart has proven a useful experimental model for CPVT in reproducing a particular clinically observed human CPVT genotype [25, 40].  $RyR2^{S/S}$  ventricular myocytes show features of altered  $\text{Ca}^{2+}$  homeostasis [15] thought to result from an increased RyR2-mediated  $\text{Ca}^{2+}$  leak reflecting an increased sensitivity of  $\text{Ca}^{2+}$  release to cytosolic though not to SR levels [ $\text{Ca}^{2+}$ ] [31]. The consequent increase in cytosolic [ $\text{Ca}^{2+}$ ] would result in increased sodium-calcium exchanger (NCX) activity whose electrogenic actions would result in triggering events including delayed after-depolarizations leading to ectopic APs that could potentially initiate ventricular arrhythmia. However, these initial studies did not explore for the presence or otherwise for arrhythmic substrate that could sustain the resulting arrhythmia.

Genetic modifications in  $RyR2$  are also associated with AF phenotypes [17, 31, 37]. This has also been modeled by the  $RyR2^{S/S}$  system which demonstrates abnormal atrial  $\text{Ca}^{2+}$  homeostasis, delayed triggering events and atrial arrhythmia [22, 48]. However, they also demonstrated reductions in conduction velocity that could provide an arrhythmic substrate [22]. This was attributed to a reduced  $\text{Na}^+$  current which could be either attributed to a reduced  $\text{Na}_v1.5$  expression or a direct inhibitory effect on  $\text{Na}^+$  channel function of altered  $\text{Ca}^{2+}$  homeostasis [21]. This could arise from either increased leak of SR  $\text{Ca}^{2+}$  or the consequently elevated diastolic  $\text{Ca}^{2+}$ . Indeed, recent evidence suggests that altered  $\text{Ca}^{2+}$  homeostasis can acutely affect cardiac excitability due to both direct [47] and indirect actions on the  $\text{Na}^+$  channel [2, 5, 41]. CaMKII has been shown to directly interact with  $\text{Na}_v1.5$ , shifting  $\text{Na}^+$  current availability to a more depolarized membrane potential, thus enhancing the accumulation of  $\text{Na}^+$  channels into an intermediate inactivated state [2]. Increases in CaMKII activity additionally is known to phosphorylate RyR2 which itself increases SR  $\text{Ca}^{2+}$  leak [45]. Intracellular  $\text{Ca}^{2+}$  concentration can also acutely modulate  $\text{Na}^+$  current density in ventricular myocytes [5]. Atrial conduction slowing has also been observed in further models of RyR2-mediated  $\text{Ca}^{2+}$  leak including a CSQ2 mutant [14, 26].

These findings suggest that altered  $\text{Ca}^{2+}$  homeostasis following the chronic atrial alterations in SR  $\text{Ca}^{2+}$  release in the  $RyR2^{S/S}$  system could compromise  $\text{Na}_v1.5$  expression or function as a result of the elevated diastolic  $\text{Ca}^{2+}$ . The present study now demonstrates that  $RyR2^{S/S}$  ventricles similarly displayed a reduced  $\text{Na}_v1.5$  expression and consequently reduced peak  $I_{\text{Na}}$ , that could explain similar reductions in their conduction velocities [49]. It further extends these findings in localizing this altered expression to the membrane, as well as the whole tissue, fraction (Fig. 7), leading to a reduced maximum rate of AP depolarization, which would be expected to reduce AP conduction velocity, thus creating an arrhythmic substrate. These findings accompanied a greater

arrhythmogenicity of  $RyR2^{S/S}$  murine ventricles, which showed arrhythmic events on extrasystolic (S2) stimulation unlike WT and more frequent arrhythmias that occurred at higher BCLs during dynamic stimulation. These findings took place despite indistinguishable AP recovery characteristics in WT and  $RyR2^{S/S}$  ventricles, as reflected in VERP and  $\text{APD}_{90}$  readings, thereby excluding re-entrant mechanisms involving recovery phases of the AP [27]. In contrast,  $RyR2^{S/S}$  showed reduced indices of conduction velocity,  $\theta'$  through all BCLs examined compared to WT, despite indistinguishable AP amplitude,  $\text{APD}_{90}$  and  $\theta'$  alternans and their variation with BCL or DI, particularly at low BCLs.

Our findings therefore suggest that the arrhythmic substrate results from reduced expression of  $\text{Na}_v1.5$  in the membrane, where a reduced  $I_{\text{Na}}$  leads to slowed AP conduction velocity, in the ventricles of  $RyR2^{S/S}$  mice. This would be consistent with a situation in which abnormalities in cytosolic  $\text{Ca}^{2+}$  exert both short- and long-term effects. In the short term, ectopic activity can follow transient elevations in cytosolic [ $\text{Ca}^{2+}$ ]. In the long term, chronic elevations in cytosolic [ $\text{Ca}^{2+}$ ] can result in a downregulation of either  $\text{Na}_v1.5$  expression or activity, thereby reducing action potential conduction and resulting in arrhythmic substrate. In such a situation, short-term triggering events could potentially form a means for initiating electrical events then perpetuated by the pre-existing arrhythmic substrate. These findings may have broader implications for the mode of therapeutic intervention in a variety of  $\text{Ca}^{2+}$  dependent, and potentially some  $\text{Na}_v1.5$  dependent, arrhythmia.

**Acknowledgments** This work was supported by Royal Society / National Science Foundation of China International Joint Project Grant (JP100994/ No.81211130599) (JAF and AM), Issac Newton Trust/ Wellcome Trust ISSF/ University of Cambridge Joint Research Grants Scheme (JAF) and by the Wellcome Trust and Medical Research Council (CLH).

**Open Access** This article is distributed under the terms of the Creative Commons Attribution 4.0 International License (<http://creativecommons.org/licenses/by/4.0/>), which permits unrestricted use, distribution, and reproduction in any medium, provided you give appropriate credit to the original author(s) and the source, provide a link to the Creative Commons license, and indicate if changes were made.

## References

- Abriel H, Zaklyazminskaya EV (2013) Cardiac channelopathies: genetic and molecular mechanisms. *Gene* 517:1–11. doi:10.1016/j.gene.2012.12.061
- Ashpole NM, Herren AW, Ginsburg KS, Brogan JD, Johnson DE, Cummins TR, Bers DM, Hudmon A (2012)  $\text{Ca}^{2+}$ /calmodulin-dependent protein kinase II (CaMKII) regulates cardiac sodium channel  $\text{Na}_v1.5$  gating by multiple phosphorylation sites. *J Biol Chem* 287:19856–19869. doi:10.1074/jbc.M111.322537
- Bezaniilla F, Armstrong CM (1977) Inactivation of the sodium channel. I. Sodium current experiments. *J Gen Physiol* 70:549–566. doi:10.1085/jgp.70.5.549

4. Bhuiyan ZA, van den Berg MP, van Tintelen JP, Bink-Boelkens MTE, Wiesfeld ACP, Alders M, Postma AV, van Langen I, Mannens MMAM, Wilde AAM (2007) Expanding spectrum of human RYR2-related disease: new electrocardiographic, structural, and genetic features. *Circulation* 116:1569–1576. doi:10.1161/CIRCULATIONAHA.107.711606
5. Casini S, Verkerk AO, van Borren MMGJ, van Ginneken ACG, Veldkamp MW, de Bakker JMT, Tan HL (2009) Intracellular calcium modulation of voltage-gated sodium channels in ventricular myocytes. *Cardiovasc Res* 81:72–81. doi:10.1093/cvr/cvn274
6. Chiamvimonvat N, Kargacin ME, Clark RB, Duff HJ (1995) Effects of intracellular calcium on sodium current density in cultured neonatal rat cardiac myocytes. *J Physiol* 483(Pt 2):307–318
7. Coppen SR, Dupont E, Rothery S, Severs NJ (1998) Connexin45 expression is preferentially associated with the ventricular conduction system in mouse and rat heart. *Circ Res* 82:232–243. doi:10.1161/01.RES.82.2.232
8. Desai KH, Sato R, Schauble E, Barsh GS, Kobilka BK, Bernstein D (1997) Cardiovascular indexes in the mouse at rest and with exercise: new tools to study models of cardiac disease. *Am J Physiol* 272:H1053–H1061
9. Di Pino A, Caruso E, Costanzo L, Guccione P (2014) A novel RyR2 mutation in a 2-year-old baby presenting with atrial fibrillation, atrial flutter, and atrial ectopic tachycardia. *Heart Rhythm* 11:1480–1483. doi:10.1016/j.hrthm.2014.04.037
10. Dobrev D (2010) Atrial Ca<sup>2+</sup> signaling in atrial fibrillation as an antiarrhythmic drug target. *Naunyn Schmiedeberg's Arch Pharmacol* 381:195–206. doi:10.1007/s00210-009-0457-1
11. Duff HJ, Offord J, West J, Catterall WA (1992) Class I and IV antiarrhythmic drugs and cytosolic calcium regulate mRNA encoding the sodium channel alpha subunit in rat cardiac muscle. *Mol Pharmacol* 42:570–574
12. Dupont E, el Aoumari A, Briand JP, Fromaget C, Gros D (1989) Cross-linking of cardiac gap junction connexons by thiol/disulfide exchanges. *J Membr Biol* 108:247–252. doi:10.1007/BF01871739
13. Faggioni M, Kryshtal DO, Knollmann BC (2012) Calsequestrin mutations and catecholaminergic polymorphic ventricular tachycardia. *Pediatr Cardiol* 33:959–967. doi:10.1007/s00246-012-0256-1
14. Glukhov AV, Kalyanasundaram A, Lou Q, Hage LT, Hansen BJ, Belevych AE, Mohler PJ, Knollmann BC, Periasamy M, Györke S, Fedorov VV (2015) Calsequestrin 2 deletion causes sinoatrial node dysfunction and atrial arrhythmias associated with altered sarcoplasmic reticulum calcium cycling and degenerative fibrosis within the mouse atrial pacemaker complex1. *Eur Heart J* 36:686–697. doi:10.1093/eurheartj/eh452
15. Goddard CA, Ghais NS, Zhang Y, Williams AJ, Colledge WH, Grace AA, Huang CL-H (2008) Physiological consequences of the P2328S mutation in the ryanodine receptor (RyR2) gene in genetically modified murine hearts. *Acta Physiol (Oxf)* 194:123–140. doi:10.1111/j.1748-1716.2008.01865.x
16. Gutstein DE, Morley GE, Tamaddon H, Vaidya D, Schneider MD, Chen J, Chien KR, Stuhlmann H, Fishman GI (2001) Conduction slowing and sudden arrhythmic death in mice with cardiac-restricted inactivation of connexin43. *Circ Res* 88:333–339. doi:10.1161/01.RES.88.3.333
17. Herron TJ, Milstein ML, Anumonwo J, Priori SG, Jalife J (2010) Purkinje cell calcium dysregulation is the cellular mechanism that underlies catecholaminergic polymorphic ventricular tachycardia. *Heart Rhythm* 7:1122–1128. doi:10.1016/j.hrthm.2010.06.010
18. Hwang HS, Nitu FR, Yang Y, Walweel K, Pereira L, Johnson CN, Faggioni M, Chazin WJ, Laver D, George AL, Cornea RL, Bers DM, Knollmann BC (2014) Divergent regulation of ryanodine receptor 2 calcium release channels by arrhythmogenic human calmodulin missense mutants. *Circ Res* 114:1114–1124. doi:10.1161/CIRCRESAHA.114.303391
19. Katz G, Shainberg A, Hochhauser E, Kurtzward-Josefson E, Issac A, El-Ani D, Aravot D, Afek A, Seidman JG, Seidman CE, Eldar M, Arad M (2013) The role of mutant protein level in autosomal recessive catecholamine dependent polymorphic ventricular tachycardia (CPVT2). *Biochem Pharmacol* 86:1576–1583. doi:10.1016/j.bcp.2013.09.012
20. King JH, Huang CLH, Fraser JA (2013) Determinants of myocardial conduction velocity: Implications for arrhythmogenesis. *Front Physiol* 4:154. doi:10.3389/fphys.2013.00154
21. King JH, Wickramarachchi C, Kua K, Du Y, Jeevaratnam K, Matthews HR, Grace AA, Huang CL-H, Fraser JA (2013) Loss of Nav1.5 expression and function in murine atria containing the RyR2-P2328S gain-of-function mutation. *Cardiovasc Res* 99:751–759. doi:10.1093/cvr/cvt141
22. King JH, Zhang Y, Lei M, Grace AA, Huang CL-H, Fraser JA (2013) Atrial arrhythmia, triggering events and conduction abnormalities in isolated murine RyR2-P2328S hearts. *Acta Physiol (Oxf)* 207:308–323. doi:10.1111/apha.12006
23. Kirchhoff S, Nelles E, Hagedorff A, Krüger O, Traub O, Willecke K (1998) Reduced cardiac conduction velocity and predisposition to arrhythmias in connexin40-deficient mice. *Curr Biol* 8:299–302. doi:10.1016/S0960-9822(98)70114-9
24. Koller ML, Riccio ML, Gilmour RF (1998) Dynamic restitution of action potential duration during electrical alternans and ventricular fibrillation. *Am J Physiol* 275:H1635–H1642
25. Laitinen PJ, Brown KM, Piippo K, Swan H, Devaney JM, Brahmabhatt B, Donarum EA, Marino M, Tiso N, Viitasalo M, Toivonen L, Stephan DA, Kontula K (2001) Mutations of the cardiac ryanodine receptor (RyR2) gene in familial polymorphic ventricular tachycardia. *Circulation* 103:485–490. doi:10.1161/01.CIR.103.4.485
26. Li N, Chiang DY, Wang S, Wang Q, Sun L, Voigt N, Respress JL, Ather S, Skapura DG, Jordan VK, Horrigan FT, Schmitz W, Müller FU, Valderrabano M, Nattel S, Dobrev D, Wehrens XHT (2014) Ryanodine receptor-mediated calcium leak drives progressive development of an atrial fibrillation substrate in a transgenic mouse model. *Circulation* 129:1276–1285. doi:10.1161/CIRCULATIONAHA.113.006611
27. Martin CA, Grace AA, Huang CL-H (2011) Refractory dispersion promotes conduction disturbance and arrhythmias in a Scn5a (+/-) mouse model. *Pflugers Arch* 462:495–504. doi:10.1007/s00424-011-0989-3
28. Matthews GDK, Guzadhur L, Grace A, Huang CL-H (2012) Nonlinearity between action potential alternans and restitution, which both predict ventricular arrhythmic properties in Scn5a +/- and wild-type murine hearts. *J Appl Physiol* 112:1847–1863. doi:10.1152/jappphysiol.00039.2012
29. Matthews GDK, Guzadhur L, Sabir IN, Grace AA, Huang CL (2013) Action potential wavelength restitution predicts alternans and arrhythmia in murine Scn5a +/- hearts. *J Physiol*. doi:10.1113/jphysiol.2013.254938
30. Matthews GDK, Martin CA, Grace AA, Zhang Y, Huang CL-H (2010) Regional variations in action potential alternans in isolated murine Scn5a (+/-) hearts during dynamic pacing. *Acta Physiol (Oxf)* 200:129–146. doi:10.1111/j.1748-1716.2010.02138.x
31. Meli AC, Refaat MM, Dura M, Reiken S, Wronska A, Wojciak J, Carroll J, Scheinman MM, Marks AR (2011) A novel ryanodine receptor mutation linked to sudden death increases sensitivity to cytosolic calcium. *Circ Res* 109:281–290. doi:10.1161/CIRCRESAHA.111.244970
32. Nattel S, Shiroshita-Takeshita A, Brundel BJM, Rivard L Mechanisms of atrial fibrillation: lessons from animal models. *Prog Cardiovasc Dis* 48:9–28. doi:10.1016/j.pcad.2005.06.002
33. Papadatos GA, Wallerstein PMR, Head CEG, Ratcliff R, Brady PA, Benndorf K, Saumarez RC, Trezise AEO, Huang CL-H, Vandenberg JI, Colledge WH, Grace AA (2002) Slowed

- conduction and ventricular tachycardia after targeted disruption of the cardiac sodium channel gene *Scn5a*. *Proc Natl Acad Sci U S A* 99:6210–6215. doi:10.1073/pnas.082121299
34. Priori SG, Chen SRW (2011) Inherited dysfunction of sarcoplasmic reticulum Ca<sup>2+</sup> handling and arrhythmogenesis. *Circ Res* 108:871–883. doi:10.1161/CIRCRESAHA.110.226845
  35. Priori SG, Napolitano C, Tiso N, Memmi M, Vignati G, Bloise R, Sorrentino V, Danieli GA (2001) Mutations in the cardiac ryanodine receptor gene (hRyR2) underlie catecholaminergic polymorphic ventricular tachycardia. *Circulation* 103:196–200. doi:10.1161/01.CIR.103.2.196
  36. Salvage SC, King JH, Chandrasekharan KH, Jafferji DIG, Guzadhur L, Matthews HR, Huang CL-H, Fraser JA (2015) Flecainide exerts paradoxical effects on sodium currents and atrial arrhythmia in murine RyR2-P2328S hearts. *Acta Physiol* 214:361–375. doi:10.1111/apha.12505
  37. Shan J, Xie W, Betzenhauser M, Reiken S, Chen B-X, Wronska A, Marks AR (2012) Calcium leak through ryanodine receptors leads to atrial fibrillation in 3 mouse models of catecholaminergic polymorphic ventricular tachycardia. *Circ Res* 111:708–717. doi:10.1161/CIRCRESAHA.112.273342
  38. Stokoe KS, Balasubramaniam R, Goddard CA, Colledge WH, Grace AA, Huang CL-H (2007) Effects of flecainide and quinidine on arrhythmogenic properties of *Scn5a*<sup>+/-</sup> murine hearts modelling the Brugada syndrome. *J Physiol* 581:255–275. doi:10.1113/jphysiol.2007.128785
  39. Sumitomo N, Sakurada H, Taniguchi K, Matsumura M, Abe O, Miyashita M, Kanamaru H, Karasawa K, Ayusawa M, Fukamizu S, Nagaoka I, Horie M, Harada K, Hiraoka M (2007) Association of atrial arrhythmia and sinus node dysfunction in patients with catecholaminergic polymorphic ventricular tachycardia. *Circ J* 71:1606–1609. doi:10.1253/circj.71.1606
  40. Swan H, Piippo K, Viitasalo M, Heikkilä P, Paavonen T, Kainulainen K, Kere J, Keto P, Kontula K, Toivonen L (1999) Arrhythmic disorder mapped to chromosome 1q42–q43 causes malignant polymorphic ventricular tachycardia in structurally normal hearts. *J Am Coll Cardiol* 34:2035–2042. doi:10.1016/S0735-1097(99)00461-1
  41. Tan HL, Kupersmidt S, Zhang R, Stepanovic S, Roden DM, Wilde AAM, Anderson ME, Balsler JR (2002) A calcium sensor in the sodium channel modulates cardiac excitability. *Nature* 415:442–447. doi:10.1038/415442a
  42. Taouis M, Sheldon RS, Duff HJ (1991) Upregulation of the rat cardiac sodium channel by in vivo treatment with a class I antiarrhythmic drug. *J Clin Invest* 88:375–378. doi:10.1172/JCI115313
  43. Tribulová N, Dupont E, Soukup T, Okruhlicová L, Severs NJ (2005) Sex differences in connexin-43 expression in left ventricles of aging rats. *Physiol Res* 54:705–708
  44. Van Veen TAB, Stein M, Royer A, Le Quang K, Charpentier F, Colledge WH, Huang CL-H, Wilders R, Grace AA, Escande D, de Bakker JMT, van Rijen HVM (2005) Impaired impulse propagation in *Scn5a*-knockout mice: combined contribution of excitability, connexin expression, and tissue architecture in relation to aging. *Circulation* 112:1927–1935. doi:10.1161/CIRCULATIONAHA.105.539072
  45. Voigt N, Li N, Wang Q, Wang W, Trafford AW, Abu-Taha I, Sun Q, Wieland T, Ravens U, Nattel S, Wehrens XHT, Dobrev D (2012) Enhanced sarcoplasmic reticulum Ca<sup>2+</sup> leak and increased Na<sup>+</sup>-Ca<sup>2+</sup> exchanger function underlie delayed afterdepolarizations in patients with chronic atrial fibrillation. *Circulation* 125:2059–2070. doi:10.1161/CIRCULATIONAHA.111.067306
  46. Webster G, Berul CI (2013) An update on channelopathies: from mechanisms to management. *Circulation* 127:126–140. doi:10.1161/CIRCULATIONAHA.111.060343
  47. Wingo TL, Shah VN, Anderson ME, Lybrand TP, Chazin WJ, Balsler JR (2004) An EF-hand in the sodium channel couples intracellular calcium to cardiac excitability. *Nat Struct Mol Biol* 11:219–225. doi:10.1038/nsmb737
  48. Zhang Y, Fraser JA, Jeevaratnam K, Hao X, Hothi SS, Grace AA, Lei M, Huang CL-H (2011) Acute atrial arrhythmogenicity and altered Ca<sup>2+</sup> homeostasis in murine RyR2-P2328S hearts. *Cardiovasc Res* 89:794–804. doi:10.1093/cvr/cvq229
  49. Zhang Y, Wu J, Jeevaratnam K, King JH, Guzadhur L, Ren X, Grace AA, Lei M, Huang CL-H, Fraser JA (2013) Conduction Slowing Contributes to Spontaneous Ventricular Arrhythmias in Intrinsically Active Murine RyR2-P2328S Hearts. *J Cardiovasc Electrophysiol* 24:210–218. doi:10.1111/jce.12015